

> whoami

Fazal Kareem

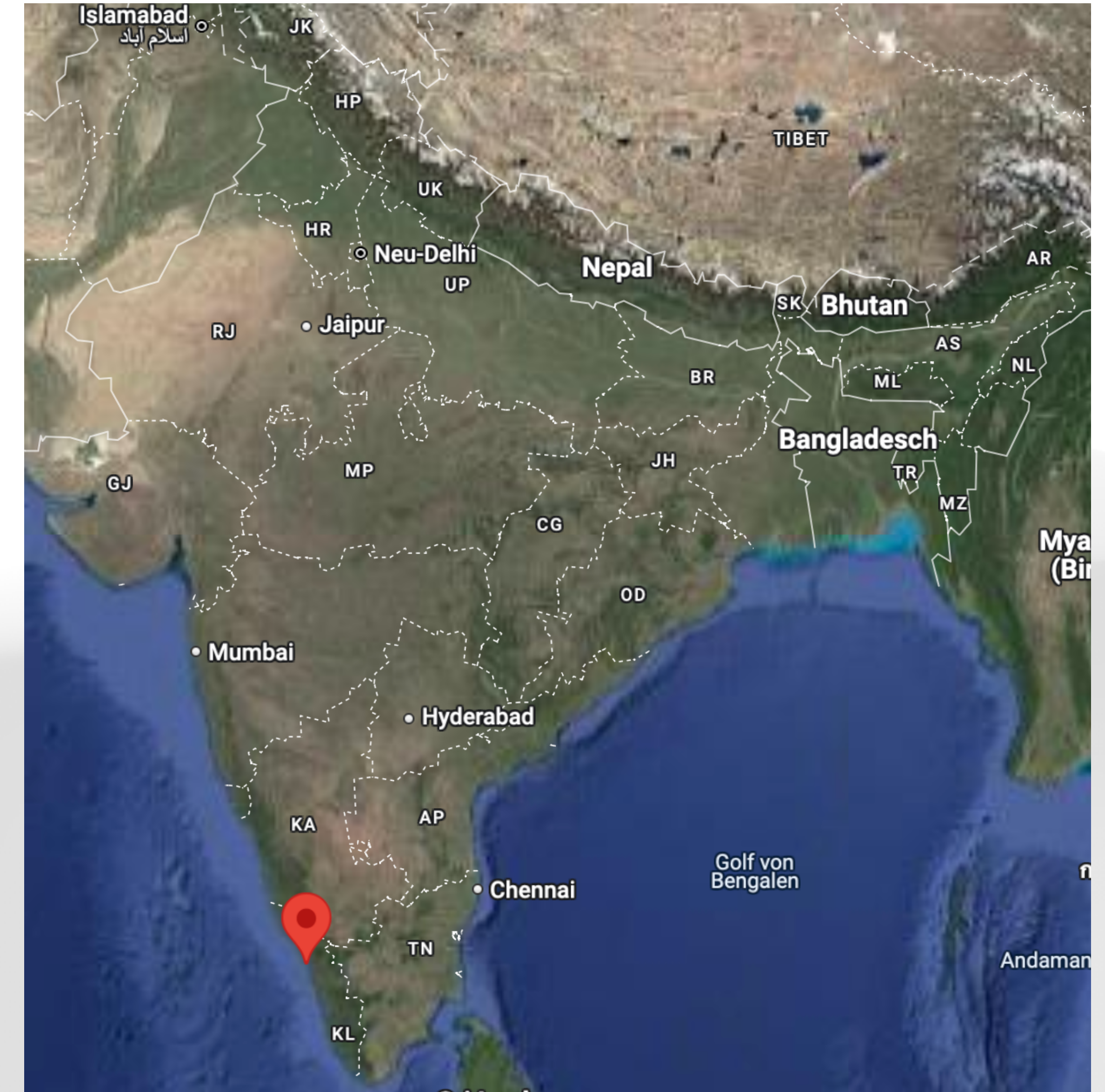
18 March 2024

Kerala

Aka — Land of coconuts :)

Aka “The gods own country”

മലയാളം — Malayalam.



Kerala

Aka – Land of coconuts :)

Aka “The gods own country”

മലയാളം – Malayalam.



Kerala

Aka — Land of coconuts :)

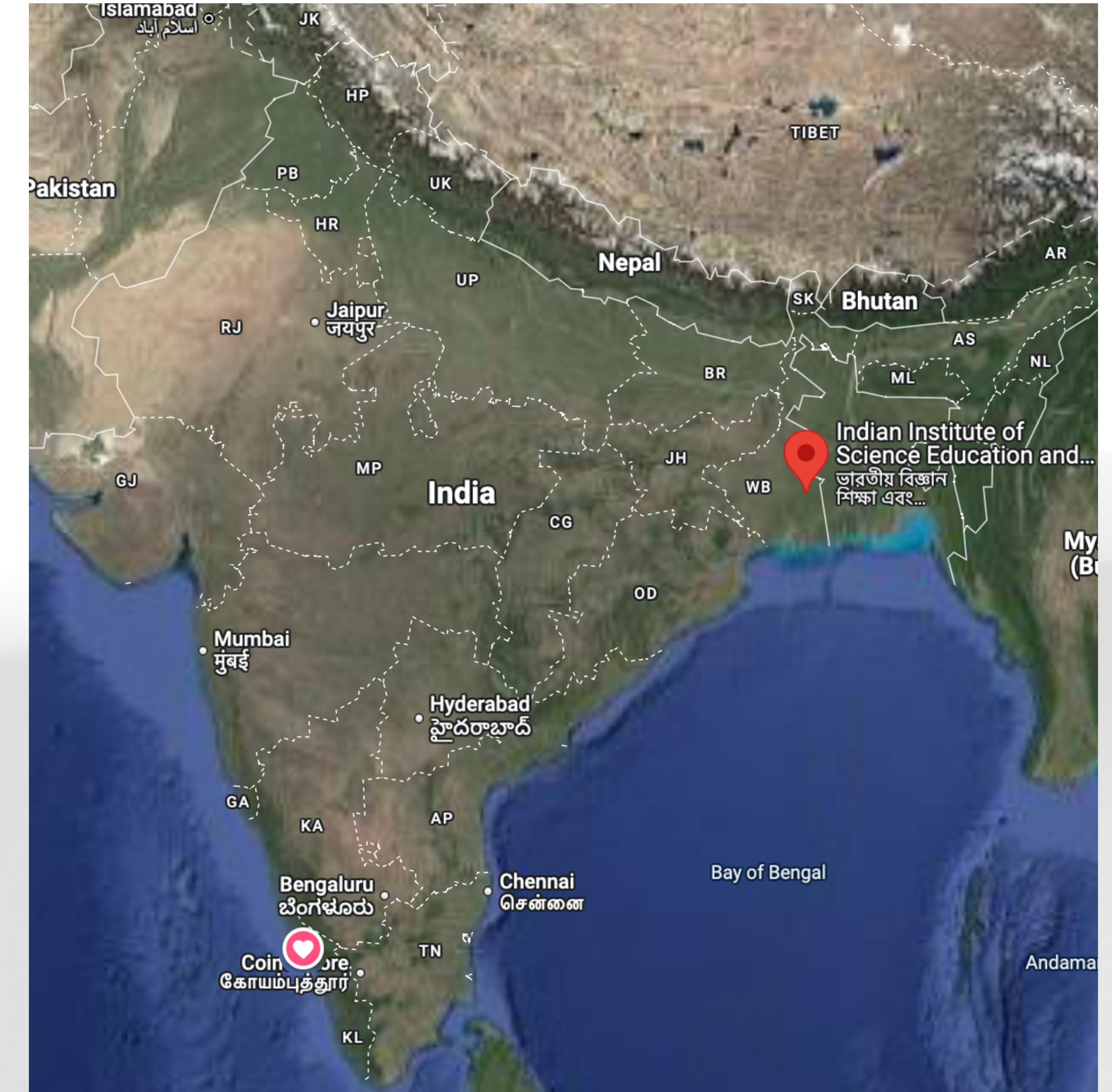
Aka “The gods own country”

മലയാളം — Malayalam.

Kolkata

BS-MS Dual degree in Physics.

IISER Kolkata



Kerala

Aka — Land of coconuts :)

Aka “The gods own country”

മലയാളം — Malayalam.

Kolkata

BS-MS Dual degree in Physics.

IISER Kolkata



Kerala

Aka – Land of coconuts :)

Aka “The gods own country”

മലയാളം – Malayalam.

Kolkata

BS-MS Dual degree in Physics.

IISER Kolkata



Kerala

Aka — Land of coconuts :)

Aka “The gods own country”

മലയാളം — Malayalam.

Kolkata

BS-MS Dual degree in Physics.

IISER Kolkata

Mumbai

Masters thesis and everything else.



Kerala

Aka — Land of coconuts :)

Aka “The gods own country”

മലയാളം — Malayalam.

Kolkata

BS-MS Dual degree in Physics.

IISER Kolkata

Mumbai

Masters thesis and everything else.



Kerala

Aka – Land of coconuts :)

Aka “The gods own country”

മലയാളം – Malayalam.

Kolkata

BS-MS Dual degree in Physics.

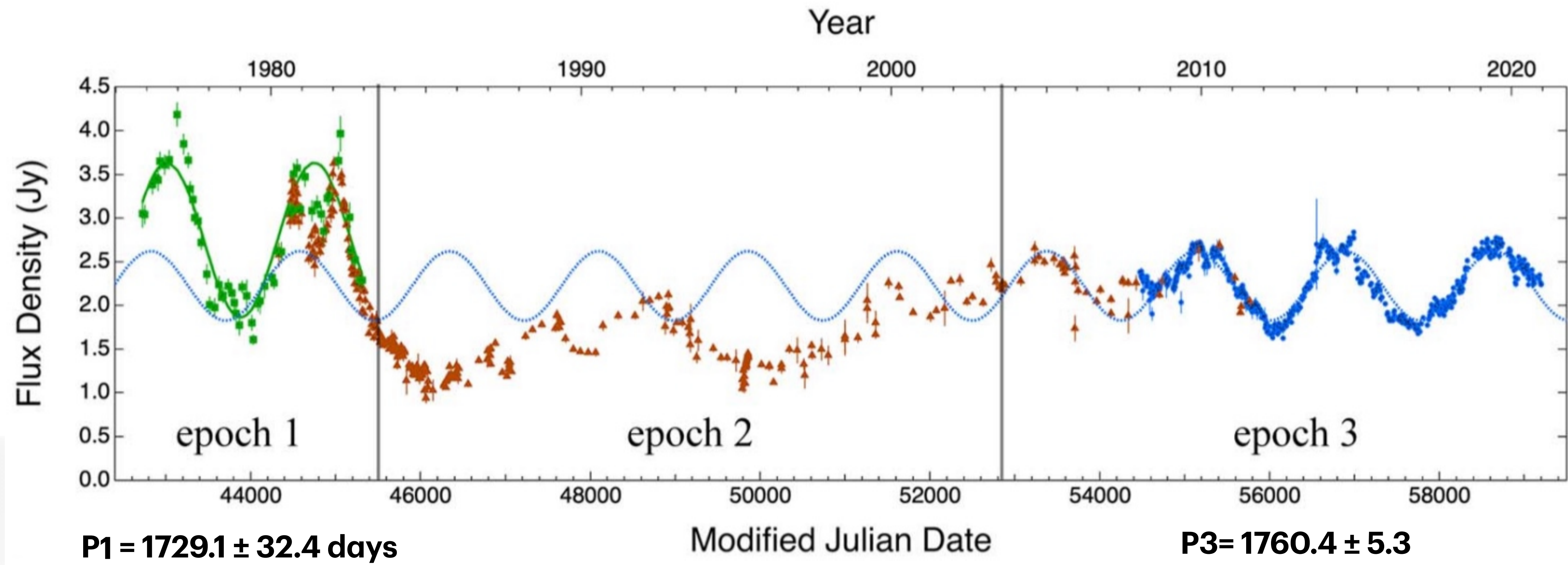
IISER Kolkata

Mumbai

Masters thesis and everything else.



Master's thesis: PKS 2131-021



Phase and periods of epoch 1 and 2 are not matching!

Master's thesis: PKS 2131-021

- Bayesian analysis of the data was done using the likelihood function:

$$\ln \mathcal{L} = -\frac{1}{2} \sum_{i=1}^N \left(\frac{(S_i - S_{\text{model},i})^2}{\sigma_i^2 + \sigma_0^2} + \ln(\sigma_i^2 + \sigma_0^2) \right).$$

- Circular Model:

$$S_{\text{model},i} = A \cos(\phi_i - \phi_0) + S_0$$

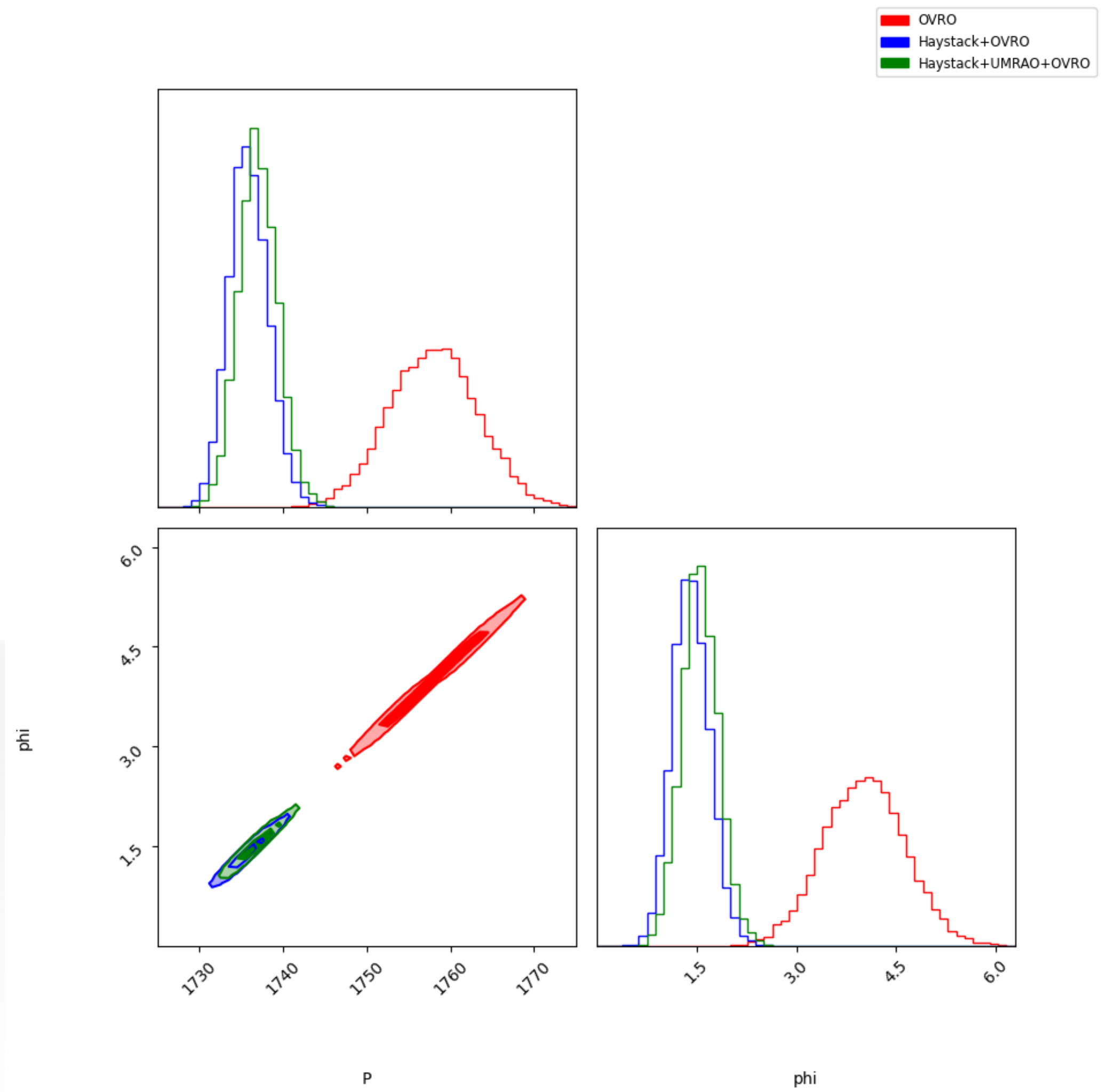
Where $\phi_i = 2\pi(t_i - t_0)/Pb$

We keep $t_0 = 51000$ fixed as in the original paper

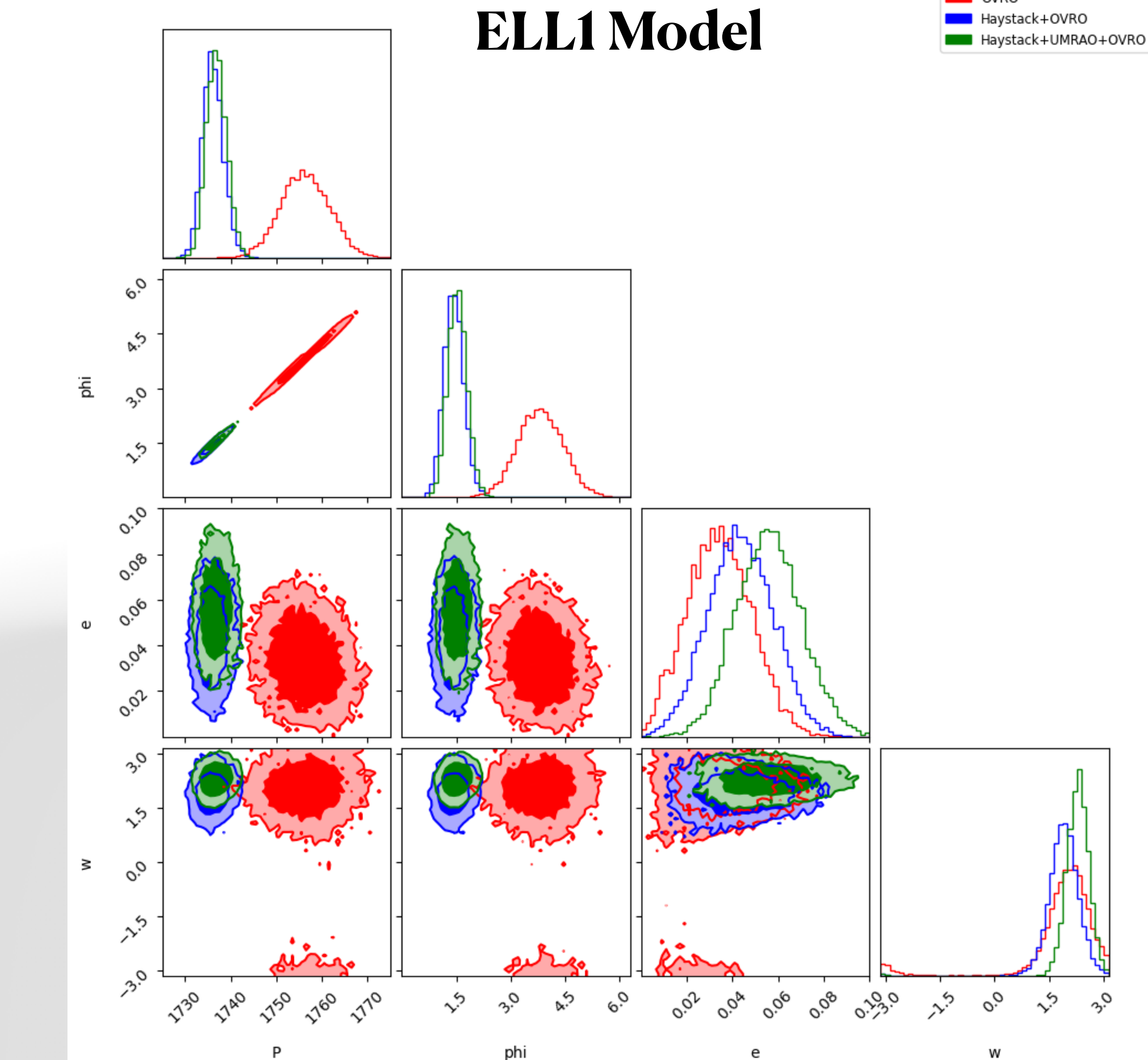
- Eccentric Model:

$$S_{\text{model},i} = A[\cos(\dot{\omega}t + \omega_0)\cos(\nu(t, n)) - \sin(\dot{\omega}t + \omega_0)\sin(\nu(t, n))] + e \cos(\dot{\omega}t + \omega_0) + S_0$$

Circular Model

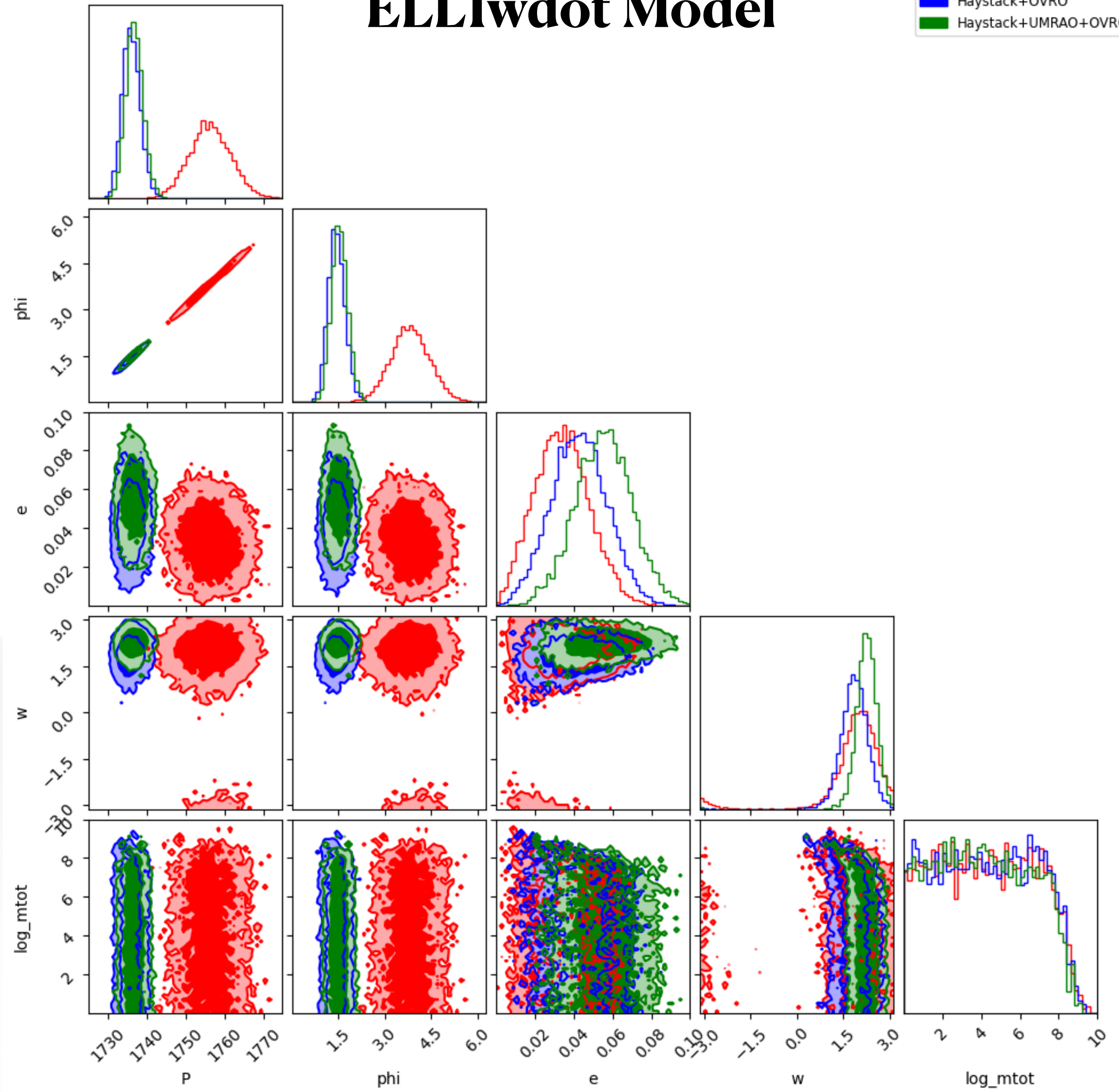


ELL1 Model



ELL1wdot Model

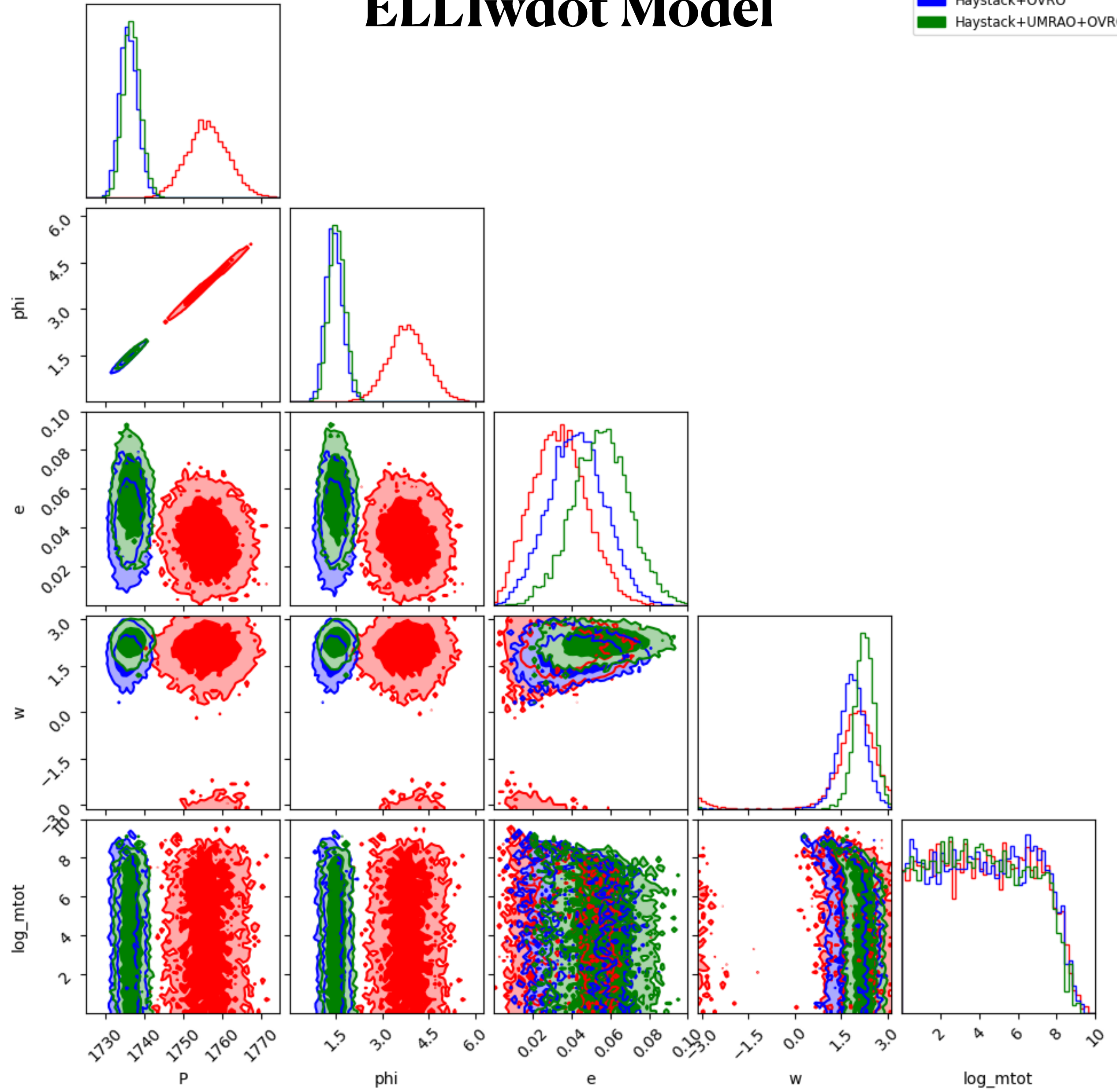
■ OVRO
■ Haystack+OVRO
■ Haystack+UMRAO+OVRO



	In(Z)	Circular	ELL1	ELL1wdot
OVRO	488.1333	486.7389	486.5839	
Haystack+OVRO	460.9094	461.2018	461.0274	
Haystack+UMRAO +OVRO	412.3386	415.4895	415.2945	

ELL1wdot Model

■ OVRO
■ Haystack+OVRO
■ Haystack+UMRAO+OVRO



	In(Z)	Circular	ELL1	ELL1wdot
OVRO	488.1333	486.7389	486.5839	
Haystack+OVRO	460.9094	461.2018	461.0274	
Haystack+UMRAO +OVRO	412.3386	415.4895	415.2945	

Total Mass $\leq 3.49 \times 10^8 M_{\odot}$

- Developed 2 pipelines for Wideband Timing of GMRT data.
 - Combined Portrait (CP)
 - Combined chi-squared (CP)

Pulsar Name	DM uncertainties (pc cm^{-3})					
	Band 3		Band 3 + 5 CC		Band 3 + 5 CP	
	Median	Minimum	Median	Minimum	Median	Minimum
J0437 – 4715	1.8×10^{-4}	1.2×10^{-4}	4.2×10^{-5}	3.7×10^{-5}	4.1×10^{-5}	3.7×10^{-5}
J0613 – 0200	7.8×10^{-5}	3.2×10^{-5}	5.6×10^{-5}	2.9×10^{-5}	6.0×10^{-5}	3.1×10^{-5}
J0751 + 1807	4.1×10^{-4}	1.9×10^{-4}	2.0×10^{-4}	1.0×10^{-4}	2.1×10^{-4}	1.0×10^{-4}
J1012 + 5307	5.9×10^{-5}	1.9×10^{-5}	3.8×10^{-5}	1.8×10^{-5}	4.0×10^{-5}	2.4×10^{-5}
J1022 + 1001	1.1×10^{-4}	4.8×10^{-5}	9.8×10^{-5}	4.8×10^{-5}	1.0×10^{-4}	4.8×10^{-5}
J1600 – 3053	2.1×10^{-4}	1.3×10^{-4}	7.8×10^{-5}	6.1×10^{-5}	8.4×10^{-5}	5.7×10^{-5}
J1643 – 1224	1.2×10^{-4}	6.4×10^{-5}	6.2×10^{-5}	3.6×10^{-5}	6.3×10^{-5}	3.4×10^{-5}
J1713 + 0747	7.3×10^{-5}	2.8×10^{-5}	3.2×10^{-5}	1.8×10^{-5}	4.1×10^{-5}	2.2×10^{-5}
J1744 – 1134	2.6×10^{-5}	1.5×10^{-5}	1.9×10^{-5}	8.7×10^{-6}	2.7×10^{-5}	1.2×10^{-5}
J1857 + 0943	2.0×10^{-4}	7.2×10^{-5}	8.7×10^{-5}	3.5×10^{-5}	9.1×10^{-5}	3.6×10^{-5}
J1909 – 3744	1.6×10^{-5}	6.7×10^{-6}	1.3×10^{-5}	6.2×10^{-6}	1.8×10^{-5}	1.2×10^{-5}
J1939 + 2134	2.8×10^{-6}	1.1×10^{-6}	2.7×10^{-6}	1.1×10^{-6}	1.7×10^{-5}	2.6×10^{-6}
J2124 – 3358	1.3×10^{-4}	2.0×10^{-5}	1.1×10^{-4}	2.0×10^{-5}	1.3×10^{-4}	2.2×10^{-5}
J2145 – 0750	3.3×10^{-5}	1.0×10^{-5}	2.5×10^{-5}	1.0×10^{-5}	2.5×10^{-5}	1.0×10^{-5}

Multiband extension of the wideband timing technique

Avinash Kumar Paladi^{1,2,★}, Churchil Dwivedi^{2,★}, Prerna Rana^{1,3}, K. Nobleson^{2,4}, Abhimanyu Susobhanan^{1,5}, Bhal Chandra Joshi^{1,6,7}, Pratik Tarafdar^{1,8}, Debabrata Deb^{1,8}, Swetha Arumugam^{1,9}, A. Gopakumar^{1,3}, M. A. Krishnakumar^{1,10,11}, Neelam Dhanda Batra^{1,12}, Jyotijwal Debnath^{1,8,13}, Fazal Kareem^{1,14,15}, Paramasivan Arumugam^{1,7}, Manjari Bagchi^{1,8,13}, Adarsh Bathula^{1,16}, Subhajit Dandapat^{1,3}, Shantanu Desai^{1,17}, Yashwant Gupta^{1,6}, Shinnouke Hisano^{1,18}, Divyansh Kharbanda^{1,17}, Tomonosuke Kikunaga^{1,18}, Neel Kolhe^{1,19}, Yogesh Maan^{1,6}, P. K. Manoharan^{1,20}, Jaikhomba Singha^{1,7}, Aman Srivastava^{1,17}, Mayuresh Surnis^{1,21} and Keitaro Takahashi^{1,22,23}

Affiliations are listed at the end of the paper

Accepted 2023 October 3. Received 2023 September 18; in original form 2023 April 25

ABSTRACT

The wideband timing technique enables the high-precision simultaneous estimation of pulsar times of arrival (ToAs) and dispersion measures (DMs) while effectively modelling frequency-dependent profile evolution. We present two novel independent methods that extend the standard wideband technique to handle simultaneous multiband pulsar data incorporating profile evolution over a larger frequency span to estimate DMs and ToAs with enhanced precision. We implement the wideband likelihood using the LIBSTEPO PYTHON interface to perform wideband timing in the TEMPO2 framework. We present the application of these techniques to the data set of 14 millisecond pulsars (MSPs) observed simultaneously in Band 3 (300–500 MHz) and Band 5 (1260–1460 MHz) of the upgraded Giant Metrewave Radio Telescope (uGMRT) with a large band gap of 760 MHz as a part of the Indian Pulsar Timing Array (InPTA) campaign. We achieve increased ToA and DM precision and sub-microsecond root mean square post-fit timing residuals by combining simultaneous multiband pulsar observations done in non-contiguous bands for the first time using our novel techniques.

Key words: gravitational waves – methods: data analysis – pulsars: general – galaxies: ISM.

1 INTRODUCTION

Pulsars are rotating neutron stars emitting broad-band electromagnetic radiation that is observed as periodic pulses. The rotation of a pulsar can be tracked accurately by measuring the times of arrival (ToAs) of its pulses, and this technique is known as pulsar timing (Edwards, Hobbs & Manchester 2006; Hobbs, Edwards & Manchester 2006). The pulsar signal is dispersed while propagating through the ionized interstellar medium (IISM) by an amount that is proportional to the integrated free electron column density along the line of sight, usually referred to as the dispersion measure (DM), and inversely proportional to the square of the observing frequency v (Lorimer & Kramer 2012). Conventionally, the rough measurement of DM for a pulsar used to be done by splitting the data into multiple sub-bands and correcting for the DM induced delay for each sub-band and then adding the dispersed bands again (Lorimer & Kramer 2012). In recent days, many sophisticated techniques have been proposed, which not only provides more accurate values of DM but also provide epoch to epoch variations of DM (e.g. Ahuja et al. 2005).

* E-mail: avinashkumarpaladi@gmail.com (AKP); churchildwivedi@gmail.com (CD)

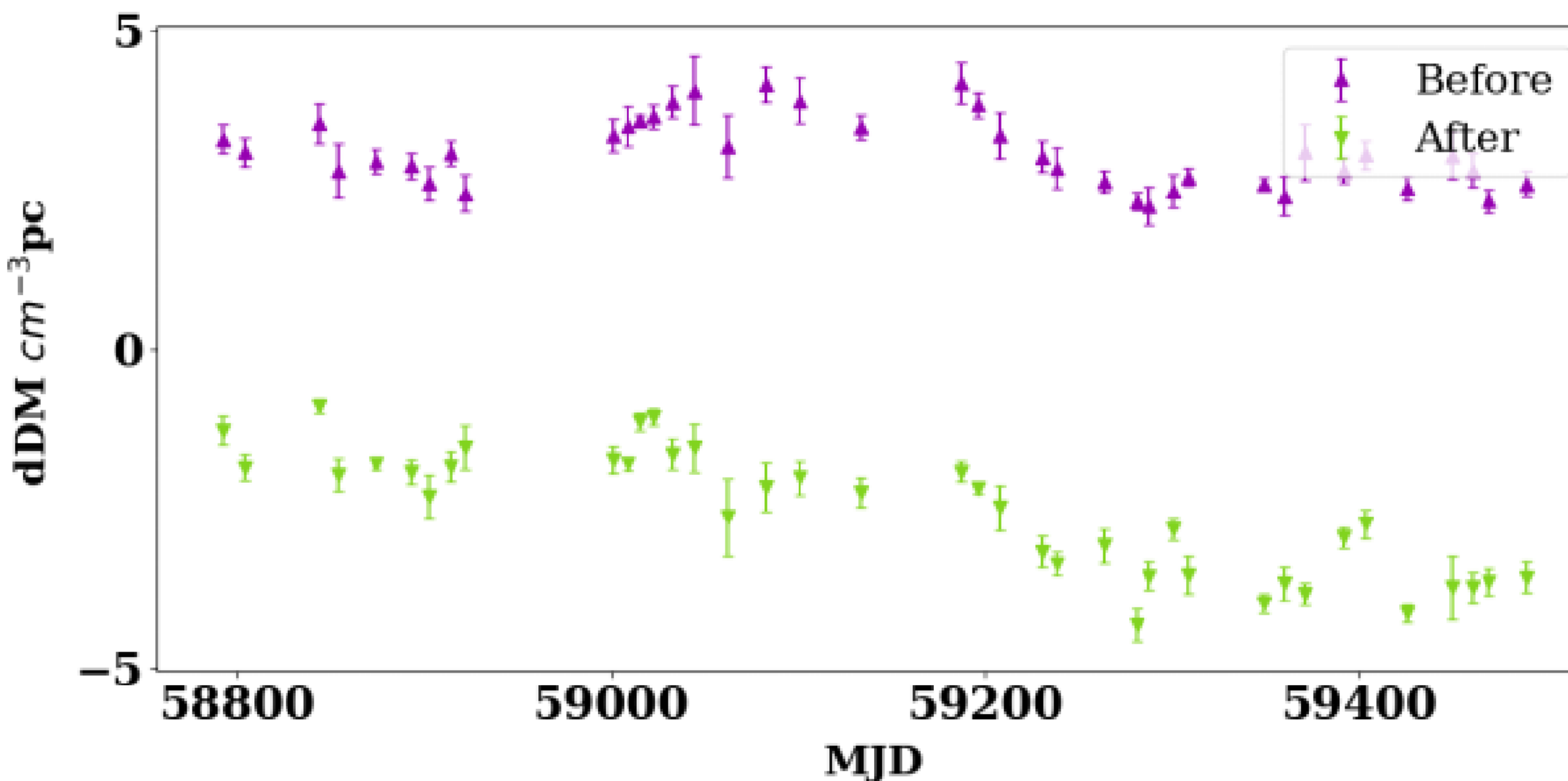
© 2023 The Author(s).

Published by Oxford University Press on behalf of Royal Astronomical Society. This is an Open Access article distributed under the terms of the Creative Commons Attribution License (<https://creativecommons.org/licenses/by/4.0/>), which permits unrestricted reuse, distribution, and reproduction in any medium, provided the original work is properly cited.

Pulsar timing has traditionally been done by splitting the data into multiple sub-bands with negligible dispersion smear and independently measuring the ToA from each sub-band, known as narrowband timing (Taylor 1992). The improvement in telescope sensitivity, the advent of wideband receivers and backends (e.g. Gupta et al. 2017; Reddy et al. 2017; Hobbs et al. 2020; Johnston et al. 2021), and decades-long pulsar timing campaigns such as Pulsar Timing Arrays (PTAs; Foster & Backer 1990) have presented significant challenges to the narrowband approach. These challenges include inadequate modelling of the pulse profile variability as a function of frequency, difficulty in correcting for interstellar scattering, and large data sizes. The wideband timing technique seeks to address these issues by treating the pulse profile as a two-dimensional (2D) entity in frequency and pulse phase (usually referred to as a *portrait*) and simultaneously measuring one ToA and one DM per observation using the full bandwidth (Pennucci, Demorest & Ransom 2014; Pennucci 2019).

PTA experiments, such as the Parkes Pulsar Timing Array (PPTA; Hobbs 2013), the European Pulsar Timing Array (EPTA; Kramer & Champion 2013), the North American Nanohertz Observatory for Gravitational Waves (NANOGrav; McLaughlin 2013), the Indian Pulsar Timing Array (InPTA; Joshi et al. 2018), the Chinese Pulsar Timing Array (CPTA; Lee 2016), MeerKat Pulsar Timing Array

- Pulsar Profile simulator to test scatter-broadening estimates.
 - Convolved a simulated intrinsic pulse with constant and varying scatter tails.
 - Injected Epoch to Epoch DM variations.
 - Developed DMScat to removed effects of scattering from the data (to an extend)



The DM time-series for the InPTA data set of PSR J1643–1224 before and after the application of the technique. Here, $d\text{DM}$ is the offset between the estimated and the fiducial DM used to align the template.

Improving DM estimates using low-frequency scatter-broadening estimates

Jaikhomba Singha   ^{1,2*}, Bhal Chandra Joshi,^{2,3} M. A. Krishnakumar,^{3,4,5} Fazal Kareem   ^{6,7}, Adarsh Bathula,⁸ Churchil Dwivedi   ⁹, Shebin Jose Jacob   ¹⁰, Shantanu Desai   ¹¹, Pratik Tarafdar   ¹², P. Arumugam,² Swetha Arumugam,¹³ Manjari Bagchi   ^{12,14}, Neelam Dhanda Batra,¹⁵, Subhajit Dandapat   ¹⁶, Debabrata Deb   ¹², Jyotijwal Debnath,^{12,14} A. Gopakumar,¹⁶ Yashwant Gupta,³, Shinnosuke Hisano,¹⁷ Ryo Kato,^{18,19} Tomonosuke Kikunaga   ^{20,21}, Piyush Marmat   ², K. Nobleson   ¹⁷, Avinash K. Paladi   ²², Arul Pandian B.   ²³, Thiagaraj Prabu,²³ Prerna Rana   ¹⁶, Aman Srivastava,¹¹, Mayuresh Surnis   ²⁴, Abhimanyu Susobhanan   ²⁵ and Keitaro Takahashi^{17,19}

Affiliations are listed at the end of the paper

Accepted 2024 October 17. Received 2024 October 16; in original form 2023 September 28

ABSTRACT

A pulsar's pulse profile gets broadened at low frequencies due to dispersion along the line of sight or due to multipath propagation. The dynamic nature of the interstellar medium makes both of these effects time-dependent and introduces slowly varying time delays in the measured times-of-arrival similar to those introduced by passing gravitational waves. In this article, we present an improved method to correct for such delays by obtaining unbiased dispersion measure (DM) measurements by using low-frequency estimates of the scattering parameters. We evaluate this method by comparing the obtained DM estimates with those, where scatter-broadening is ignored using simulated data. A bias is seen in the estimated DMs for simulated data with pulse-broadening with a larger variability for a data set with a variable frequency scaling index, α , as compared to that assuming a Kolmogorov turbulence. Application of the proposed method removes this bias robustly for data with band averaged signal-to-noise ratio larger than 100. We report the measurements of the scatter-broadening time and α from analysis of PSR J1643–1224, observed with upgraded Giant Metrewave Radio Telescope as part of the Indian Pulsar Timing Array experiment. These scattering parameters were found to vary with epoch and α was different from that expected for Kolmogorov turbulence. Finally, we present the DM time-series after application of this technique to PSR J1643–1224.

Key words: pulsars: general – pulsars: individual (PSR J1643–1224) – ISM: general.

1 INTRODUCTION

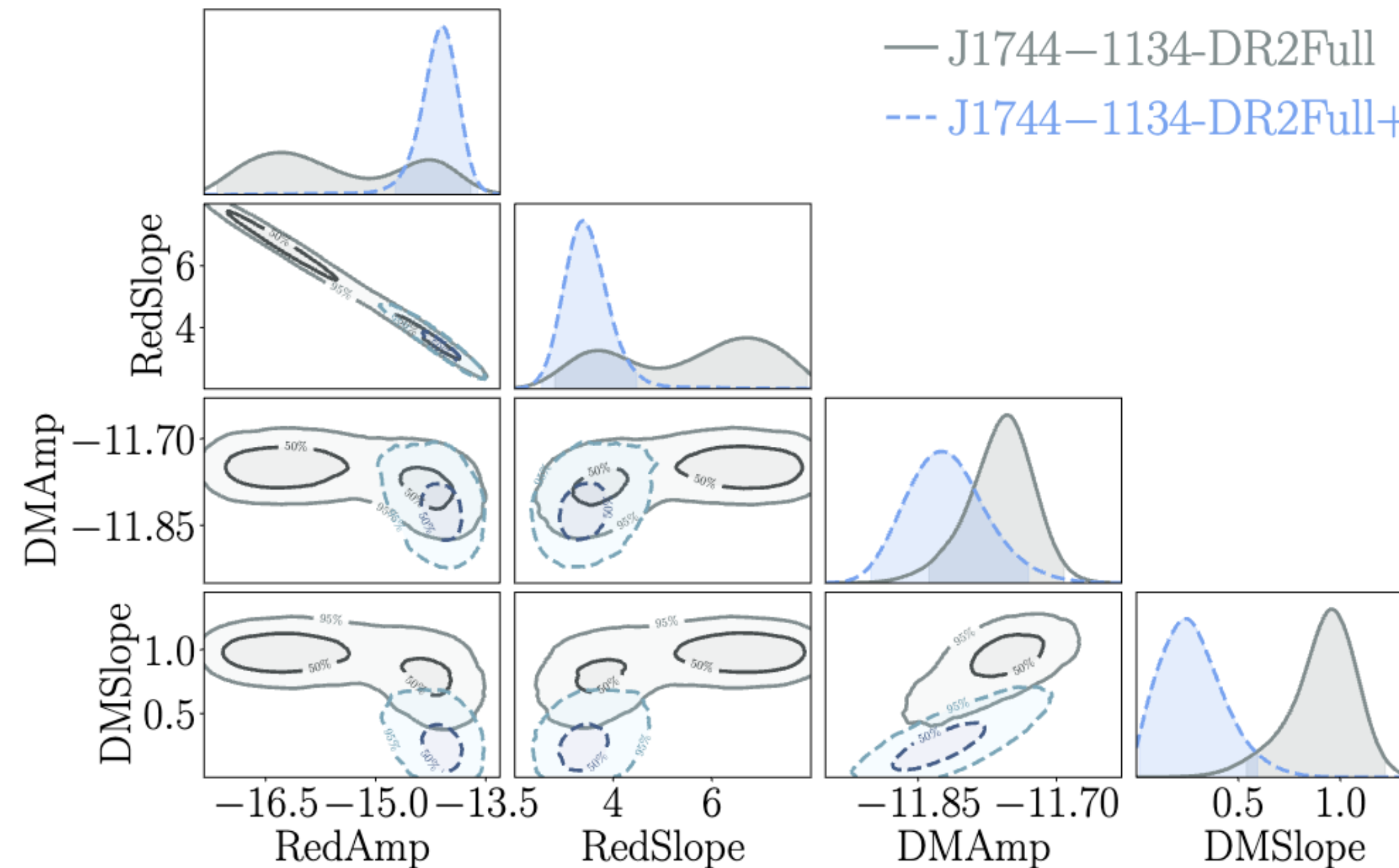
The precision in the time of arrival (ToA) of a pulsar's radio pulse is determined, in part, by how bright and sharp the received pulse is. Both of these quantities, namely the signal-to-noise ratio (S/N) and the pulse width, are affected by the propagation of the pulsed signal through the ionized interstellar medium (IISM). The IISM can impose a frequency-dependent delay on the pulses, which, when added together without proper correction, will make the pulse appear smeared. This dispersion is mainly caused by the integrated column density of electrons along the line of sight and is quantified by the dispersion measure (DM). In addition, electron density inhomogeneities in the IISM encountered along the line of sight lead to multipath propagation of radio waves, which also broadens the pulse (Rickett 1977). This pulse broadening can be mathematically described as a convolution of the intrinsic pulse profile with a pulse broadening function, such as $\exp(-\phi/\tau_{sc})$, where ϕ is the pulse phase

and τ_{sc} is the scatter-broadening time-scale in the case of a thin scattering screen (Williamson 1972). Different methods have been proposed in literature in order to obtain the scatter-broadening time-scales. Several fitting techniques have been used (Löhmer et al. 2001, 2004; Krishnakumar et al. 2015; Geyer et al. 2017; Krishnakumar, Joshi & Manoharan 2017; Krishnakumar et al. 2019) to estimate pulse broadening parameters for a sample of pulsars. Multiple works (Bhat et al. 2004; Kirsten et al. 2019; Young & Lam 2024) have used techniques based on the CLEAN (Högbom 1974; Bhat, Cordes & Chatterjee 2003) algorithm. The scatter-broadening time-scales can also be estimated using scintillation bandwidth (Cordes, Weisberg & Boriakoff 1985). A complementary method uses cyclic spectroscopy (CS) (Demorest 2011) to determine the impulse response function of the interstellar medium (ISM) and thereby estimating pulse broadening times (Walker, Demorest & van Straten 2013).

Both the phenomena, scattering and dispersion, are time-variable due to the dynamic nature of IISM. This variation induces a slowly varying chromatic time delay in the ToA measurements. The time-scale of this stochastic delay is similar to that of the gravitational wave (GW) signature arising from an isotropic stochastic gravitational

* E-mail: mjaikhomba@gmail.com, jaikhomba.singha@uct.ac.za

The second data release from the European Pulsar Timing Array

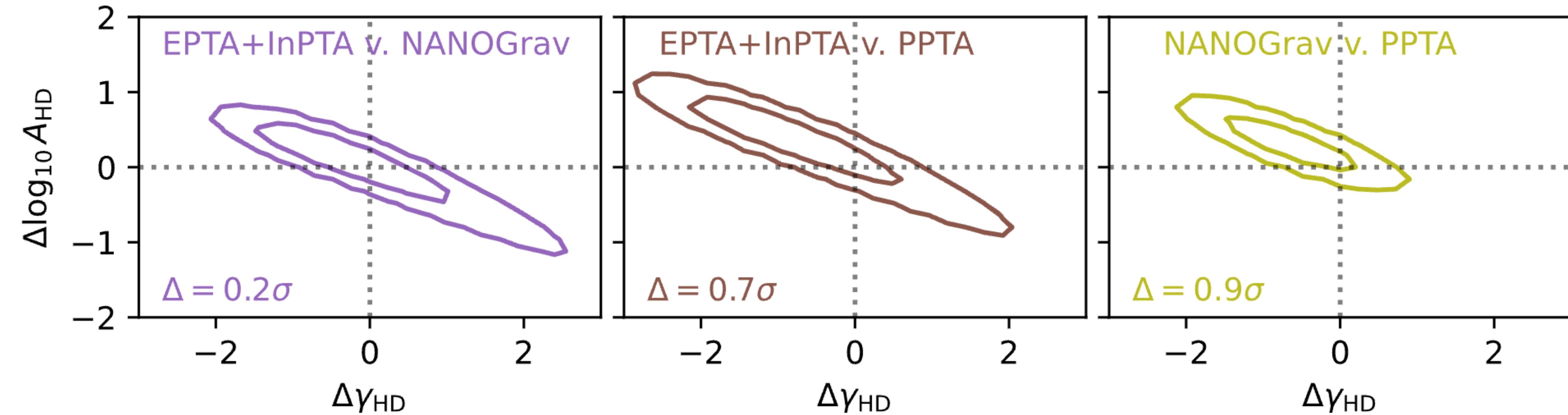


Red and DM noise models for PSR J1744–1134 using DR2full and DR2full+ datasets. The inclusion of InPTA data allows a better constraint on the achromatic noise.

Pulsar	Model	RN-RN	DM-DM
J0613–0200	DM+RN	0.74	2.97
J0751+1807	DM	X	0.63
J1012+5307	DM+RN	0.02	0.04
J1022+1001	DM+RN	0.08	0.52
J1600–3053	DM	X	4.64
J1713+0747	DM+RN	0.01	0.14
J1744–1134	DM+RN	0.20	2.29
J1857+0943	DM	X	0.05
J1909–3744	DM+RN	0.05	4.39
J2124–3358	DM	X	0.84

Estimated tension (Z-score in sigma) between the DR2full and DR2full+ datasets for the red and DM noise models.

Comparing PTA Results on the n-Hz StochasticGW Background



Difference distributions for GWB parameters between pairs of PTAs as computed by tensiometer

Now I'm here :)

Now I'm here :)

- ▶ Finding fast spinning and COMPACT binary pulsars

Now I'm here :)

- ▶ Finding fast spinning and COMPACT binary pulsars
- ▶ Follow up and timing of known Relativistic Binary pulsars

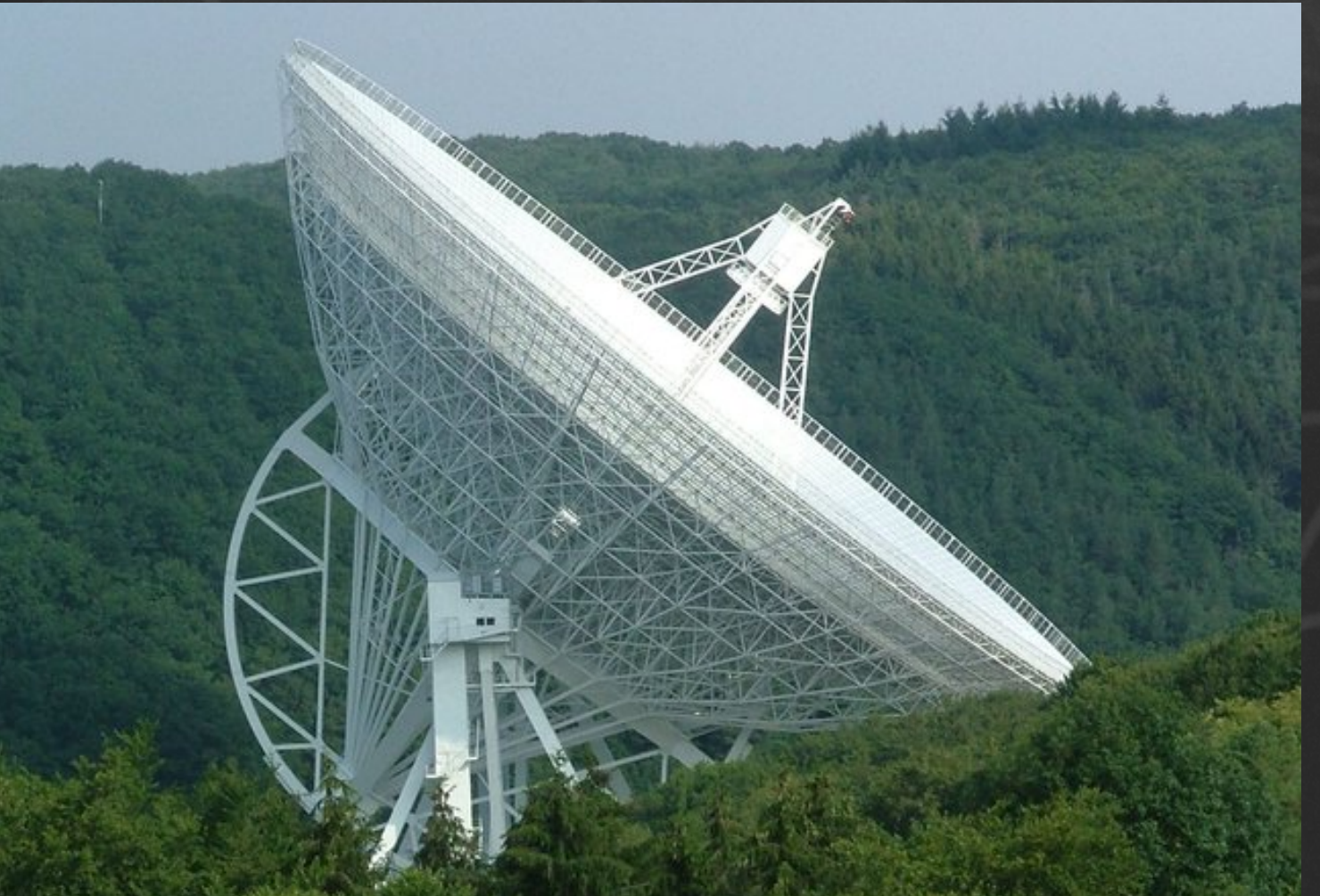
Now I'm here :)

- ▶ Finding fast spinning and COMPACT binary pulsars
- ▶ Follow up and timing of known Relativistic Binary pulsars
- ▶ Tests of GR and Alternative theories of Gravity with these pulsar systems

Now I'm here :)

- ▶ Finding fast spinning and COMPACT binary pulsars
- ▶ Follow up and timing of known Relativistic Binary pulsars
- ▶ Tests of GR and Alternative theories of Gravity with these pulsar systems

COMPACT - EFFELSBERG



RelBin



TRAPUM GC

Project 1: COMPACT - Effelsberg

Cluster Name	RA (h:m:s)	DEC (dd:mm:ss)	Distance (kpc)	DM YMW16 (pc/cc)	DM NE2001 (pc/cc)	DM PSR (pc/cc)	Rise LST (h:m:s)	Set LST (h:m:s)
NGC 6355	17:23:58.60	-26:21:12.0	8.6	177.2	362.8		15:38:32	18:37:08
NGC 6544	18:07:20.13	-24:59:53.6	2.58	91.7	115.1	135	16:15:18	19:29:02
NGC 6626	18:24:32.90	-24:52:11.5	5.37	145.7	206.4	120	16:31:57	19:47:01
Terzan 5	17:48:04.85	-24:46:44.6	6.62	299.3	435.1	238	15:55:06	19:11:06
NGC 6284	17:04:28.83	-24:45:53.3	14.21	140.4	320.0		15:11:26	18:27:35
NGC 1904	05:24:11.00	-24:31:27.9	13.08	53.1	50.3		03:30:06	06:48:44
UKS 1	17:54:27.20	-24:08:43.0	15.58	812.1	981.8		15:58:45	19:22:52
VVV-CL001	17:54:42.51	-24:00:53.0	8.08	585.7	498.2		15:58:27	19:25:10
NGC 6401	17:38:36.53	-23:54:34.6	7.44	201.3	340.1		15:41:54	19:10:42
NGC 6656	18:36:23.94	-23:54:17.1	3.3	89.9	117.4	90	16:39:40	20:08:34
NGC 6325	17:17:59.13	-23:46:03.6	7.53	129.6	245.8		15:20:41	18:52:13
NGC 6642	18:31:54.23	-23:28:32.2	8.05	155.3	266.1		16:33:23	20:10:25
NGC 7099	21:40:22.11	-23:10:47.5	8.46	28.3	41.2	25	19:40:37	23:23:01
NGC 6093	16:17:02.42	-22:58:33.9	10.34	75.5	107.4		14:16:28	18:02:27
Terzan 12	18:12:15.80	-22:44:31.0	5.17	265.7	292.8		16:10:44	20:00:15
NGC 6287	17:05:09.34	-22:42:28.8	7.93	108.3	196.9		15:03:29	18:53:29
NGC 6717	18:55:06.05	-22:42:05.3	7.52	105.9	182.2		16:53:24	20:43:29
NGC 6235	16:53:25.36	-22:10:38.8	11.94	105.4	168.8		14:49:37	18:46:56
NGC 6864	20:06:04.75	-21:55:16.2	20.52	55.6	76.4		18:01:15	22:02:01
NGC 5897	15:17:24.40	-21:00:36.4	12.55	48.6	60.6		13:08:44	17:21:38
2MASS-GC02	18:09:36.51	-20:46:44.0	5.5	730.6	418.3		15:59:55	20:15:44
VVV-CL160	18:06:57.00	-20:00:40.0	6.8	951.2	562.4		15:53:54	20:18:35
2MASS-GC01	18:08:21.81	-19:49:47.0	3.37	218.8	181.4		15:54:32	20:21:15
NGC 6333	17:19:11.79	-18:30:58.5	8.3	116.4	203.8		14:59:52	19:40

Project 1: COMPACT - Effelsberg : So far.

Project 1: COMPACT - Effelsberg : So far.

- Discovery potential

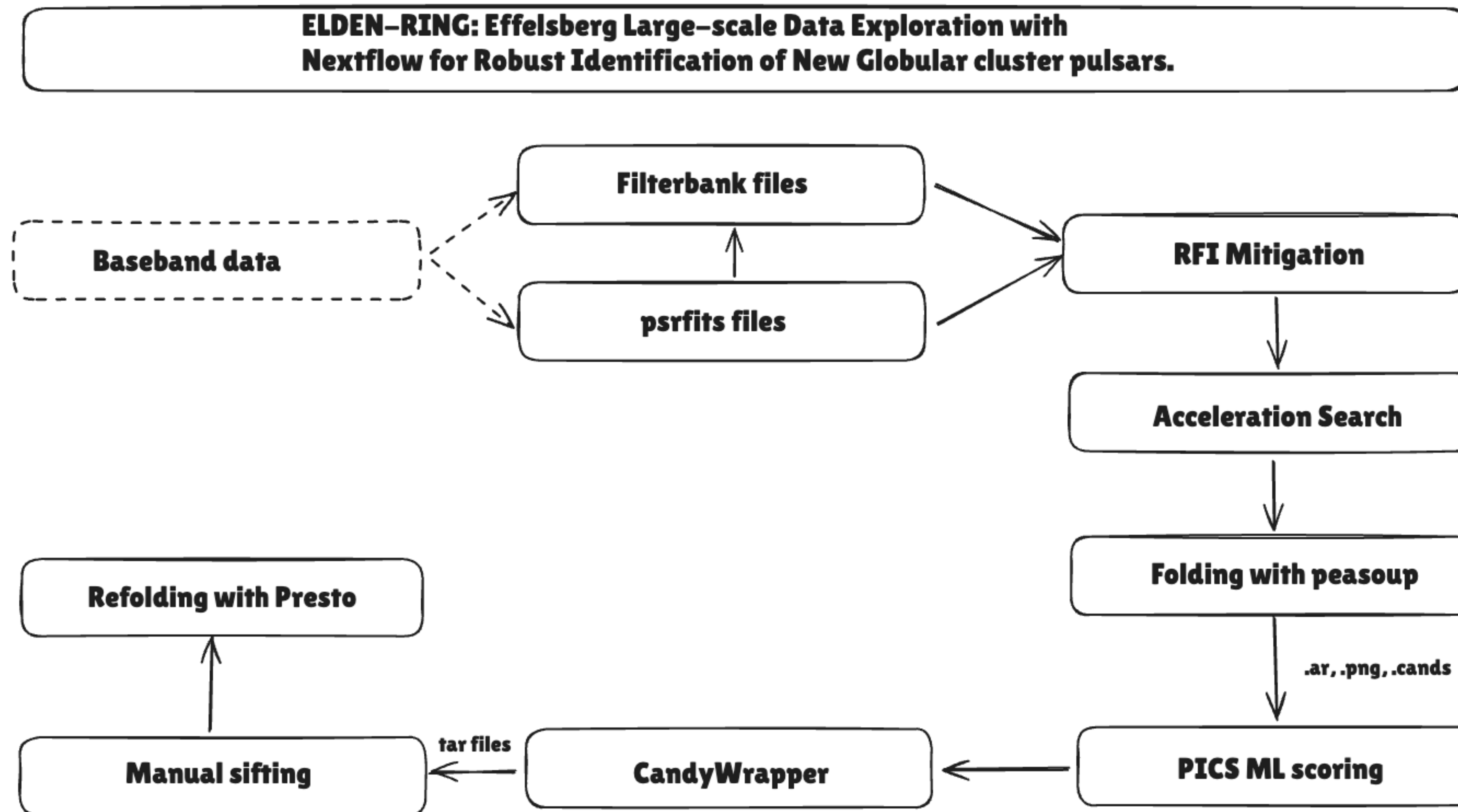
Project 1: COMPACT - Effelsberg : So far.

► Discovery potential

Globular Cluster	Known Pulsars	Detection with Effelsberg UBB				
		Band 1	Band 2	Band 3	Band 4	Band 5
TERZAN 5	49	20	13	7	6	8 (1 only detected in band 5)
NGC7099	2 Ecc redback	0	0	0	0	0
NGC6544	2	2	-	-	-	-
NGC6626	14	6 $1+2 \Rightarrow 7 (>\text{snr})$	3	2	1	4(very low snr)
NGC6656	2	2	1	1	0	0

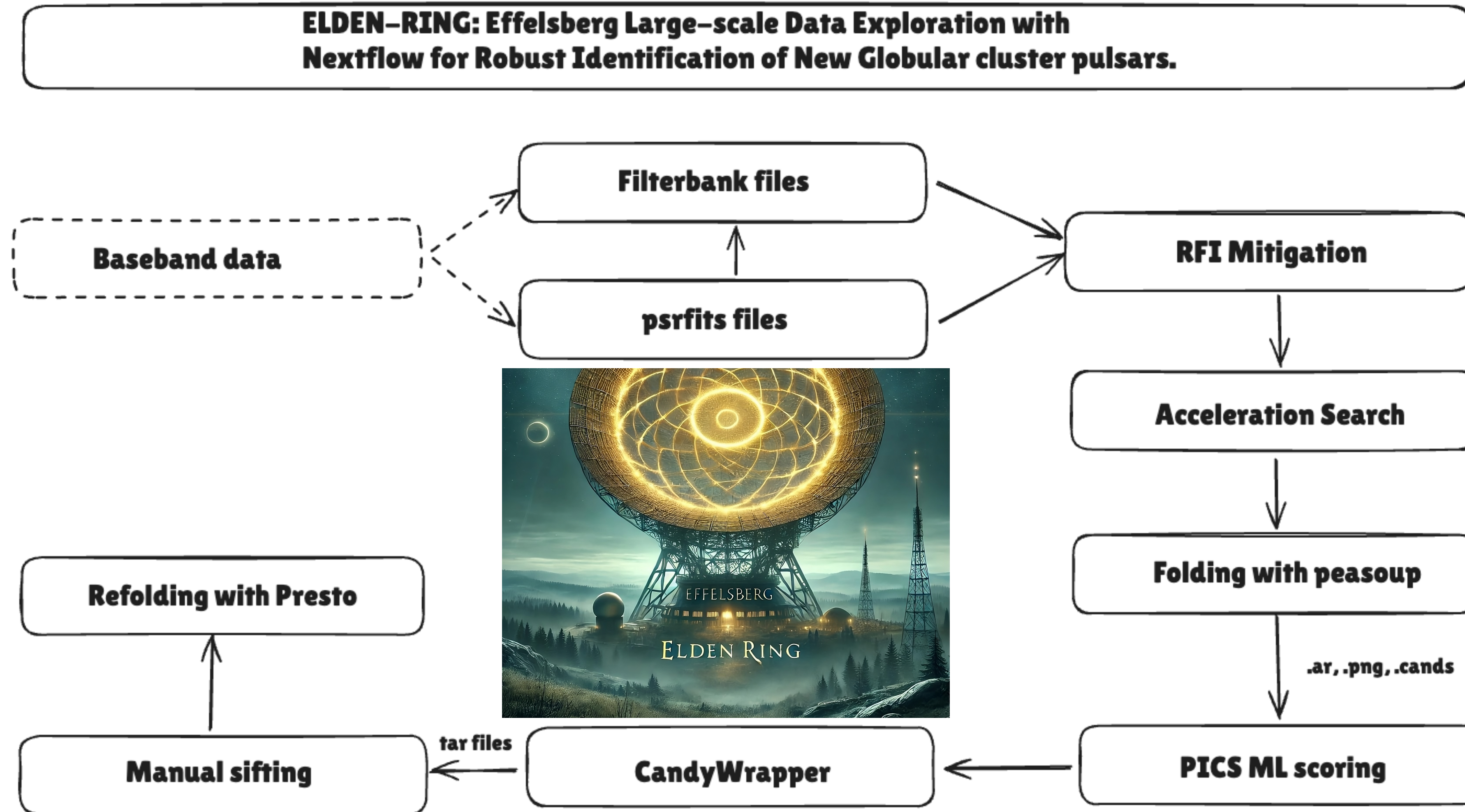
Project 1: COMPACT - Effelsberg : So far.

► Data processing pipeline



Project 1: COMPACT - Effelsberg : So far.

► Data processing pipeline

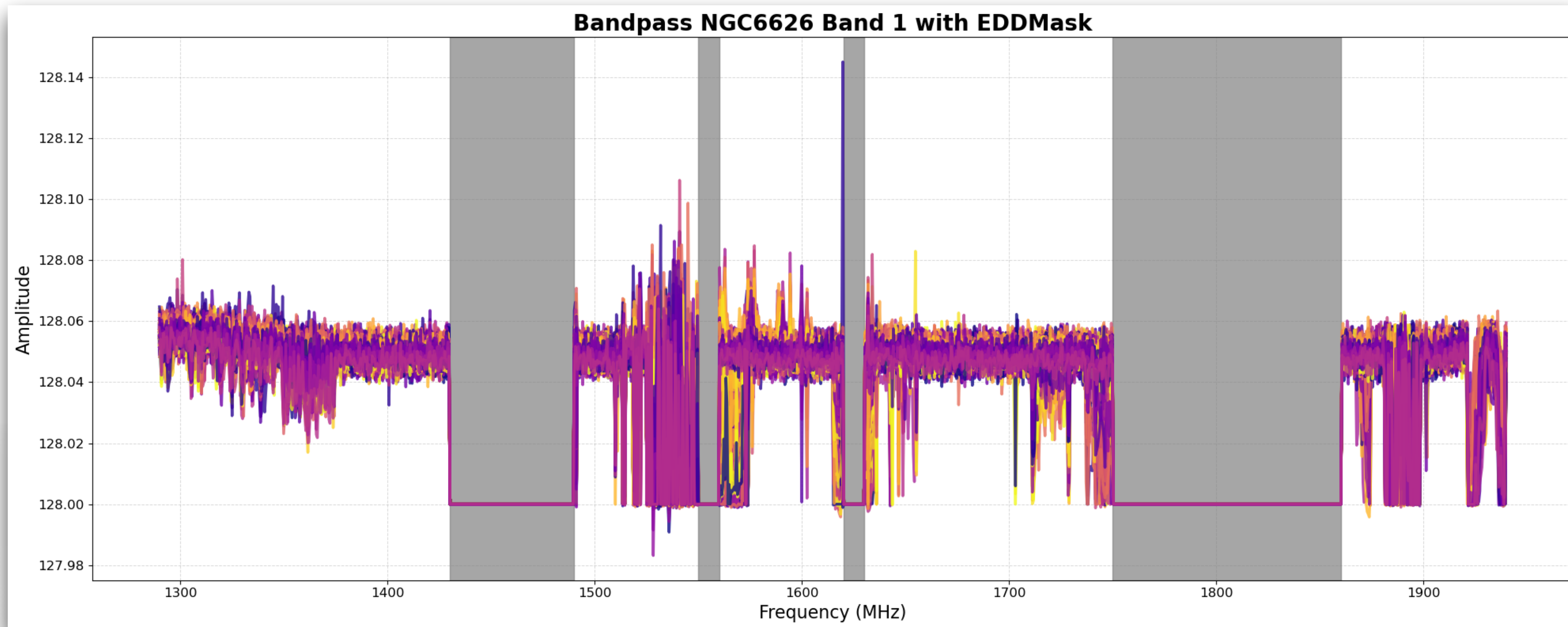


Project 1: COMPACT - Effelsberg : So far.

- RFI Mitigation

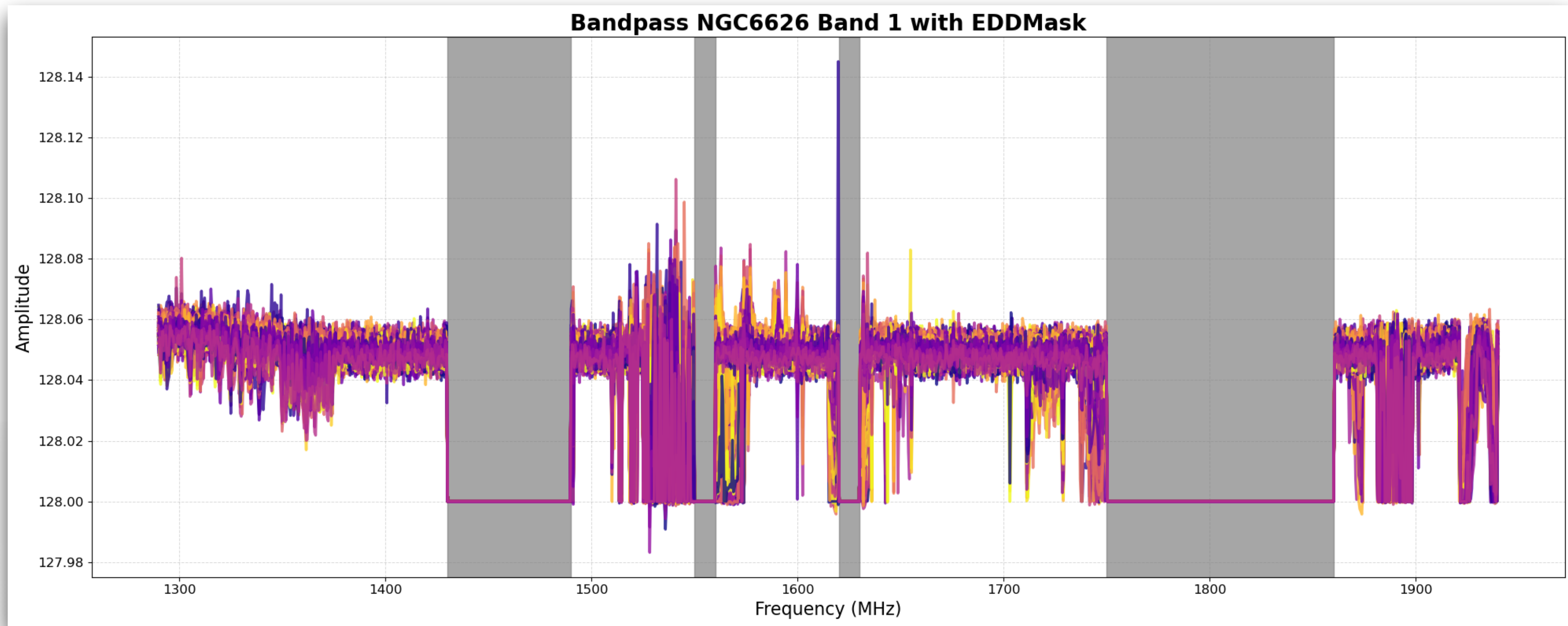
Project 1: COMPACT - Effelsberg : So far.

► RFI Mitigation



Project 1: COMPACT - Effelsberg : So far.

► RFI Mitigation



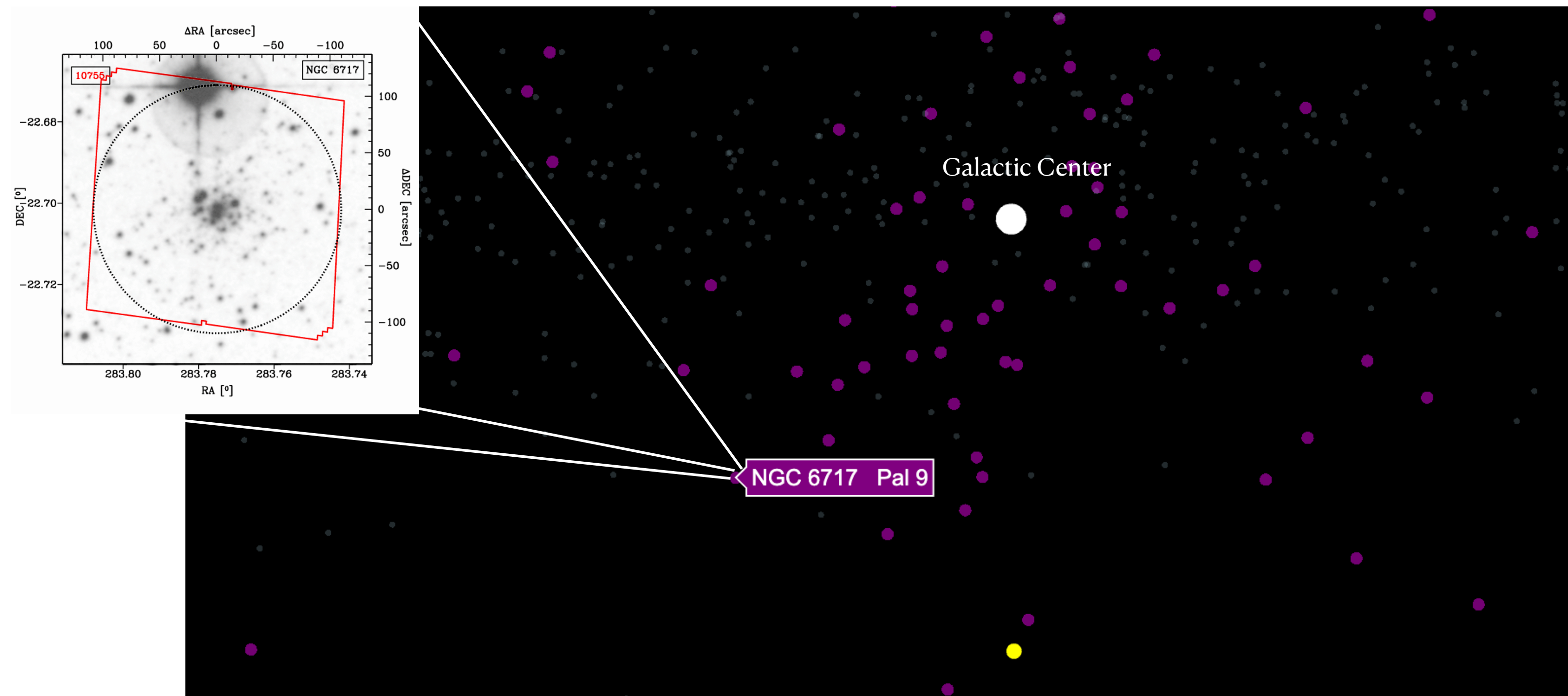
EDD Masks and the current RFI Mitigation softwares are not enough for RFI mitigation

Project 2 : TRAPUM-GC Search - NGC6717

At a distance of 7.52 kpc

Discovered in 1784

In the constellation Sagittarius



```
> whoami
```

Python

```
def end_talk():
    print("Process finished with exit code 0. Thanks for listening!")
```

```
end_talk()
```

Eccentric Model

$$\vec{\beta}_1 \cdot (\hat{n} - \vec{\beta}) \sim \vec{\beta}_1 \cdot \theta \hat{\theta} = \theta_x \beta_x + \theta_y \beta_y + \theta_z \beta_z$$

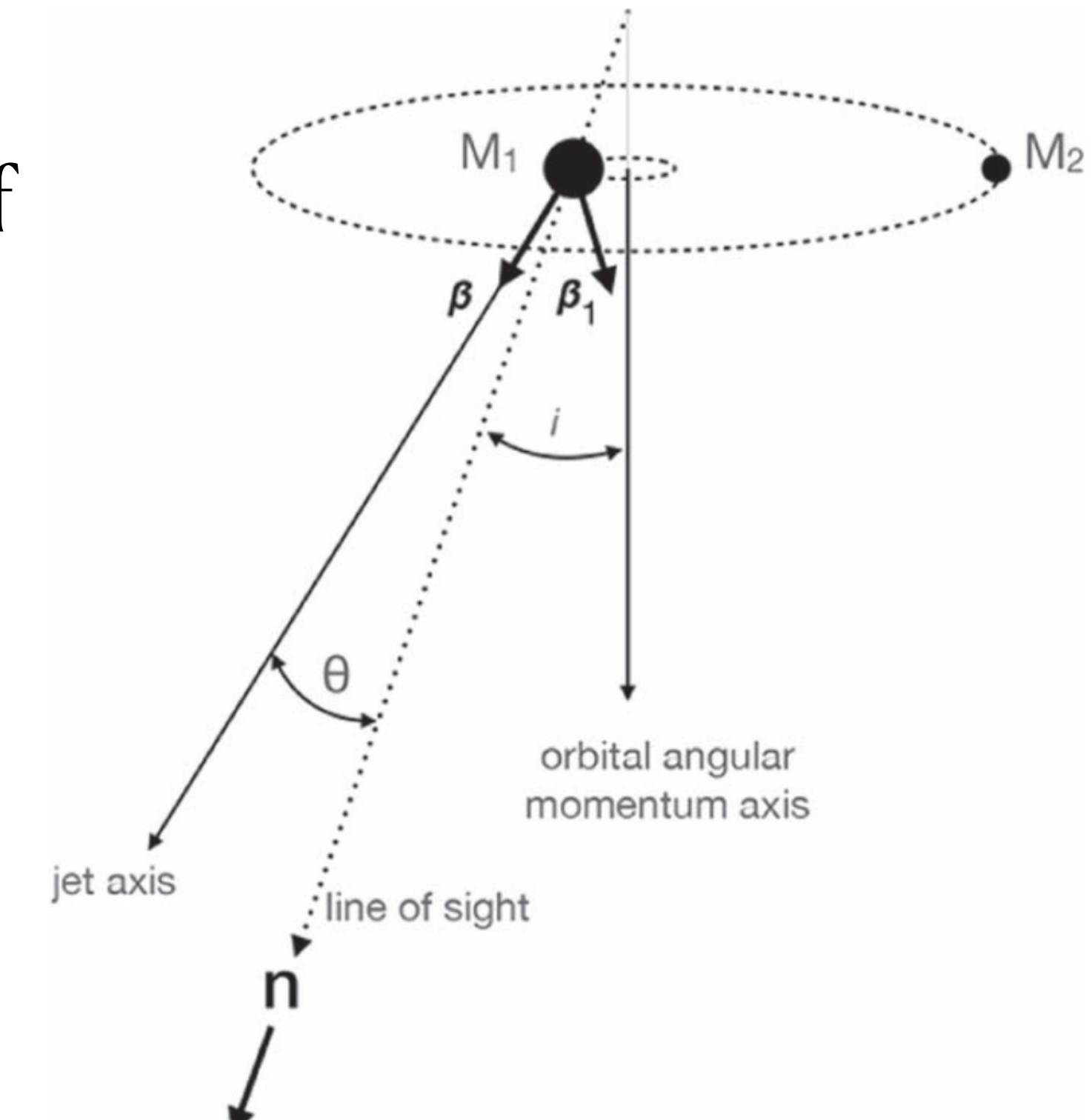
The orbital velocity of BH in case of eccentricity and advance of periastron in the astrocentric coordinate system can be derived as:

$$\beta_y = \frac{2\pi a}{P\sqrt{1-e^2}} [\cos(\dot{\omega}t + \omega_0 + \nu) + e \cos(\dot{\omega}t + \omega_0)]$$

ν = true anomaly $\dot{\omega}$ = periastron advance

$$\beta_y \theta = B[\cos(\dot{\omega}t + \nu + \omega) + e \cos(\dot{\omega}t + \omega)] \theta$$

This can be rewritten by separating the cosines.



$E = u$ = eccentric anomaly

$f = \nu$ = true anomaly

$M = l$ = Mean anomaly = $n(t - t_0)$

Eccentric Model

$$\delta S/S = A_0 [\cos(\dot{\omega}t + \omega)\cos(\nu(t, n)) - \sin(\dot{\omega}t + \omega)\sin(\nu(t, n)) + e \cos(\dot{\omega}t + \omega)]$$

$$A_0 = \frac{2\pi a}{P\sqrt{1-e^2}} \frac{2\gamma^2\theta(2-\alpha)}{(1+\gamma^2\theta^2)} \cos i$$

$$n = \frac{2\pi}{P} - \text{ mean angular velocity}$$
$$l = n(t - t_0) - \text{ mean anomaly}$$

In this equation $\cos(\nu)$ and $\sin(\nu)$ can be rewritten in terms of mean anomaly $l = n(t - t_0)$ using Bessel functions to the second order approximation:

$$\cos(\nu(n, t)) = -e + \frac{2(1-e^2)}{e} \sum_{r=1}^{\infty} J_r(re) \cos(rn(t - t_0)) \quad J(re) - \text{Bessel function of first kind}$$

$$\sin(\nu(n, t)) = 2\sqrt{1-e^2} \sum_{r=1}^{\infty} \frac{1}{r} \left(\frac{d}{de} J_r(re) \right) \sin(rn(t - t_0)) \quad e - \text{eccentricity}$$

Eccentric Model

$$\text{Cos}(\nu(n, t)) = -e + \frac{2(1 - e^2)}{e} \sum_{r=1}^{\infty} J_r(re) \text{Cos}(rn(t - t_0))$$

$$\text{Sin}(\nu(n, t)) = 2\sqrt{1 - e^2} \sum_{r=1}^{\infty} \frac{1}{r} \left(\frac{d}{de} J_r(re) \right) \text{Sin}(rn(t - t_0))$$

$$S = A[\text{Cos}(\dot{\omega}t + \omega)\text{Cos}(\nu(t, n)) - \text{Sin}(\dot{\omega}t + \omega)\text{Sin}(\nu(t, n))] + e \text{Cos}(\dot{\omega}t + \omega) + S_0$$

- We can use the obtained $\dot{\omega}$, e , and n to constraint the total mass of the system using the equation

$$\dot{\omega} = \frac{3}{1 - e^2} \times \left(\frac{GM}{c^3} \right)^{2/3} \times \left(\frac{2\pi}{P} \right)^{5/3}$$

ELL1 Model

- Since the eccentricity is very low, instead of searching for e and w , we can use the first and second Laplace–Lagrange (LL) parameters and time of ascending node (T_Ω)
- These parameters, namely $\epsilon_1 = e \sin \omega$, $\epsilon_2 = e \cos \omega$, and $T_\Omega = T_0 - \omega/n$

where n is the mean motion, replace the regular Keplerian parameters e , ω , and T_0

$$\Delta S = A \left(\cos \Phi + \frac{\epsilon_1}{2} (\cos 2\Phi + 1) + \frac{\epsilon_2}{2} \sin 2\Phi \right)$$

$$\Phi = l + w = n(t - T_0 + \frac{w}{n}) = n(t - T_\Omega)$$

Secular variation of ϵ_1 and ϵ_2

$$\epsilon_1 = \epsilon_{10} + \dot{\epsilon}_1 (t - T_\Omega) \quad \epsilon_2 = \epsilon_{20} + \dot{\epsilon}_2 (t - T_\Omega)$$

For small $\dot{\omega}\tau$,

$$\epsilon_1(t) = \epsilon_{10} + \epsilon_{20}\dot{\omega}\tau$$

$$\epsilon_2(t) = \epsilon_{20} - \epsilon_{10}\dot{\omega}\tau$$

$$\dot{\omega} = K n$$